Journal of Nuclear Materials 389 (2009) 101–107

Contents lists available at ScienceDirect

Journal of Nuclear Materials

journal homepage: www.elsevier.com/locate/jnucmat

Thermodynamic study of the U–Si system

A. Berche [a,*], C. Rado [b], O. Rapaud [b], C. Guéneau [a], J. Rogez [c]

[a] DEN/DANS/DPC/SCP - CEA Saclay, 91191 Gif-sur-Yvette, Cedex, France
[b] DEN/DTEC/SDTC - CEA Marcoule, 30207 Bagnols-sur-Cèze, Cedex, France
[c] CNRS, IM2NP (UMR 6242), Aix-Marseille Université, FST Saint-Jérôme, France

ABSTRACT

The uranium–silicon phase diagram is a key system to predict the possible interaction between the fuel kernel (U, Pu)C and the inert matrix SiC considered for the gas-cooled fast reactor systems. The experimental data from the literature on the uranium–silicon system are critically reviewed. Differential Thermal Analysis experiments are carried out to measure the temperatures of the phase transitions in the composition range 6–46% at Si. The experimental results are compared to the available data of the literature. The microstructure of the samples has been analysed using scanning electron microscopy. In view of the analyses, some solidification paths are proposed. Finally, the present experimental results and the available data of the literature have been used to perform a thermodynamic modelling of the uranium–silicon system using the CALPHAD method.

1. Introduction

The present work takes part of the FUELBASE project for the development of a thermodynamic database for advanced nuclear fuel materials. For the Gas-cooled Fast Reactor, the carbides (U, Pu)C and SiC are considered as candidate materials for respectively the fuel kernel and the inert matrix [1–3]. The high level of the operating temperature of the fuel materials requires the prediction of the phase diagrams and the thermodynamic properties of the U–Pu–Si–C quaternary system. Among the binary sub-systems, the U–Si system is a key system to assess. The experimental data available in the literature will be reviewed. The new experimental results obtained by Differential Thermal Analysis will then be presented. Finally a thermodynamic assessment using the CALPHAD method will be proposed.

2. Bibliographic study and selection of the data for the assessment

The phase diagram reported in Massalski's compilation [4] is presented in Fig. 1.

The U–Si system is characterized by the existence of several intermetallic compounds: Si_3U, Si_2U, $Si_{1.88}U$, Si_5U_3, SiU, Si_2U_3 and SiU_3. The present phase diagram is based on the investigations by Kaufmann et al. [5] who determined the phase equilibria using thermal analysis, heat treatments, metallography and X-ray diffraction and from Vaugoyeau's work et al. [6] who investigated the phase diagram from 30 to 60 at.% U by performing heat treatments in two-phase domains and thermal analysis to determine liquidus temperatures. The compounds $Si_{1.88}U$, Si_5U_3 and SiU were found to exhibit a narrow composition range by Vaugoyeau et al. [6], which was not taken into account in our own thermodynamic assessment of the system. The compound U_5Si_4 has been elaborated and characterized by X-ray diffraction for the first time by Noel et al. [7]. The temperature range of stability of this compound is unknown. In this work, $Si_{1.88}U$ is considered instead of Si_2U. In fact, the simultaneous existence of both $Si_{1.88}U$ and Si_2U is not clearly established. The allotropic transition for the SiU_3 compound quoted by Blum et al. [8] was not considered. Finally, the limit of solubility of silicon in uranium was measured by Shunk [9], Straatmann and Neumann [10].

The enthalpies of formation of the intermetallic compounds have been measured by Gross et al. [12] and O'Hare et al. [13] using calorimetry. Alcock and Grieveson [14] measured silicon vapour pressure above the mixtures USi–U_3Si_5, U_3Si_5–USi_2, USi_2–USi_3 and USi_3–Si from the weight loss of a Knudsen cell. From these measurements, the Gibbs energy of U_3Si_5, USi_2 and USi_3 were directly derived. Activities of uranium and silicon for the U–U_3Si_2 mixture were determined from the chemical analysis of the condensate formed from the vapour effusing from the cell. In case of small values of uranium activity, for the U_3Si_2–USi mixture, a solid/liquid equilibration method using liquid gold–uranium alloys was used. The Gibbs energy of formation of the compounds was derived from the silicon and uranium activity measurements. An overall good agreement is found between all the measurements. The thermodynamic properties have been estimated by Rand and Kubaschewski [15]. All the data on enthalpies of formation are listed in Table 1.

---

[*] Corresponding author. Tel.: +33 1 69 08 62 92; fax: +33 1 69 08 92 21.
E-mail address: alexandre.berche@cea.fr (A. Berche).

0022-3115/$ - see front matter © 2009 Published by Elsevier B.V.
doi:10.1016/j.jnucmat.2009.01.014

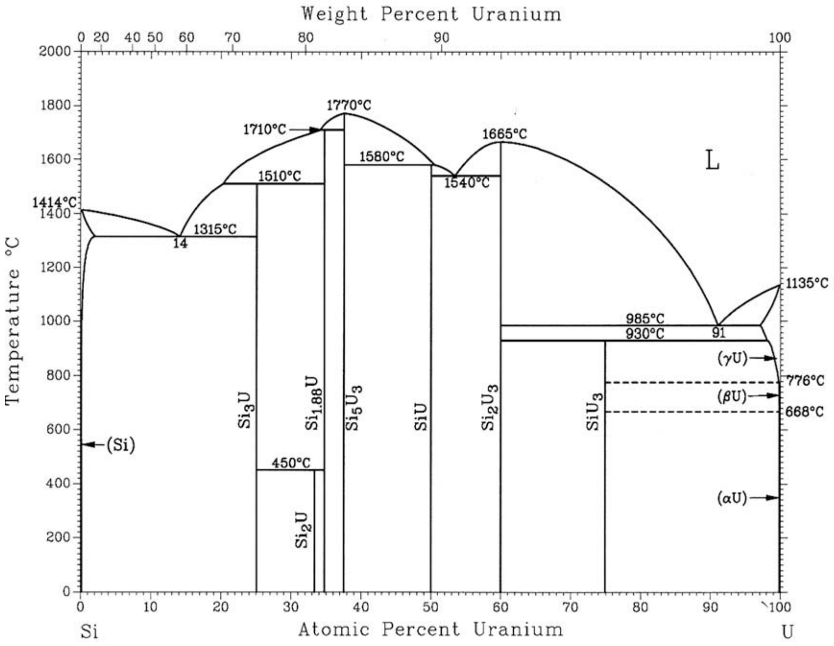

Fig. 1. Si–U phase diagram given in handbook.

Table 1
Composition, mass and mass variation of the elaborated alloys; measured temperature of transition compared to the bibliographic data.

Composition (at.% Si)		Sample mass (mg)	Mass variation		Temperature (K)			Type of reaction	Refs.
	Real		(mg)	(%)	Literature	Exp – this work	This work – assessment		
0	0	459.5	0.3	0.07	1408	1405 ± 3	–	Congruent	–
4	3.97	556.3	0.7	0.13	1258	1267 ± 3	1250	Eutectic	[11]
					1363	1340 ± 5	1360	Liquidus	[4]
9	8.69	495.1	0.6	0.12	1258	1261 ± 3	1250	Eutectic	[11]
46	46.32	269.4	0.5	0.19	1813	1820 ± 5	1840	Eutectic	[6]
					–	1867 ± 15	1860	Liquidus	–
75	74.68	132.1	−2.3	−1.74	1783	–	–	Peritectic	[11]
					?	–	–	Liquidus	–

For the optimization, direct combustion calorimetry experiments performed by Gross et al. [12] were chosen for all the compounds except U_3Si, for which the data of O'Hare et al. [13] were used. Direct combustion was preferred to both tellurium reaction calorimetry and activity measurements because of the better precision of the results. Silicon partial pressure and silicon and uranium activity measurements of Alcock and Grieveson were also used [14]. For the liquid phase, no experimental data are available. Mixing enthalpies estimated by Miedema et al. [16] were considered as a starting point to have an order of magnitude for the mixing enthalpy in the liquid for the optimization.

3. Experimental

The alloys have been directly elaborated from pure metallic uranium (99.9% purity) and silicon (99.9995%) in the furnace of the DTA apparatus. Prior to weighting the metals, the oxidation layer was chemically dissolved using nitric acid for uranium or hydrofluoric acid for silicon. The elaboration was performed by maintaining the elements during 30 min in the liquid phase. The sample was then slowly cooled. The composition, mass and mass loss of the samples synthesized and analysed in this work are presented in Table 2.

DTA measurements were performed using the SETARAM apparatus TG-DTA-92 (2400). During the analysis, a constant flow of

Table 2
Enthalpies of formation of the U_xSi_y compounds.

Phase	ΔH_f (kJ/mol at.%) 298 K	Method	References
USi_3	−33.02 ± 0.13	Direct comb.calorimetry	[12]
	−32.19 ± 0.84	Te calorimetry	[12]
	−35.53 ± 4.18	Activity meas.	[14]
	−32.60	Estimation	[15]
	−**32.90**	**Modelling**	This work
USi_2	−43.47 ± 0.42	Direct comb. calorimetry	[12]
	−42.64 ± 1.25	Te calorimetry	[12]
	−43.89 ± 4.18	Activity meas	[14]
	−43.19	Estimation	[15]
	−**43.33**	**Modelling**	This work
U_3Si_5	−44.26	Estimation	[15]
	−**42.9**	**Modelling**	This work
USi	−40.13 ± 0.84	Direct comb. calorimetry	[12]
	−43.47 ± 1.67	Te calorimetry	[12]
	−41.8 ± 4.18	Activity meas	[14]
	−42.22	Estimation	[15]
	−**41.18**	**Modelling**	This work
U_3Si_2	−33.86 ± 0.42	Direct comb. calorimetry	[12]
	−35.95 ± 3.34	Activity meas.	[14]
	−34.11	Estimation	[15]
	−**34.32**	**Modelling**	This work
U_3Si	−26.02 ± 4.8	Fluorine bomb calorimetry	[13]
	−22.99	Estimation	[15]
	−**24.93**	**Modelling**	This work

0.6 l/h of pure (more than 99.9999% volume) argon gas was maintained. The crucible used was made of Y_2O_{3-x}. The hypo-stoichiometry in oxygen allowed the crucible to absorb oxygen molecules by a getter effect. The crucible was closed by a lid in order to minimize possible vaporization of silicon. To determine the transition temperature at the thermodynamic equilibrium (rate = 0), the temperature was measured at several different rates on heating or cooling as shown in Fig. 2. On heating, the temperature of an invariant phase transition was taken at the onset of the peak whereas for monovariant transitions (liquidus), the temperature at the maximum of the heat flow peak was chosen. On cooling, the phase transition temperatures were systematically analysed at the onset of the heat flow peaks. The temperature was measured by a tungsten rhenium W-5%Re/W-26%Re thermocouple. The calibration of the measurements was performed by using pure metals Ag, Au, Ni and Pd.

SEM and EDS analyses were used to determine the composition of the different phases in the cooled samples.

The measured temperatures of phase transition for each sample are compared to literature data in Table 2.

No reactivity between the alloy and the crucible was noticed for the samples containing 4 and 9 at.% Si. In case of the sample with 46 at.% Si, a reaction layer of about 6 μm was formed between the Y_2O_{3-x} crucible and the sample. EDS analysis showed that this layer was constituted mainly of uranium and yttrium. In this case, the layer thickness was neglected in comparison with the volume of the sample. The reaction was more important for the U-75 at.% Si sample. The liquid alloy overflowed from the crucible. Such an important reaction did not allow considering the DTA measurements performed on this alloy composition. Other type of materials crucible such as ZrO_2, MgO or dense graphite could constitute better candidates for high silicon enriched alloys.

3.1. U-4 at.% Si alloy

The eutectic temperature of transition 'liquid = U_3Si_2 + bcc-U' was measured at 1267 ± 3 K in this alloy. This temperature is 9 K higher than the value proposed in the literature by Katz and Rabinowitch [11]. This slight variation could be explained by the low intensity of the eutectic transition observed on our DTA curves. The liquidus transition was measured at 1340 ± 5 K. This value was obtained at 20 K below the temperature extrapolated from the phase diagram proposed by [4].

3.2. U-9 at.% Si alloy

The presence of a liquidus transition was not detected on the DTA thermograms. The temperature of the eutectic transition 'liquid = U_3Si_2 + bcc-U' was measured at 1261 ± 3 K. This temperature corresponds to the value proposed by Katz and Rabinowitch [11]. The optical micrographs show a typical eutectic structure (Fig. 3). SEM analyses show that the microstructure is more complex (Fig. 4). In fact, the U_3Si_2 precipitates are surrounded by a layer made of the U_3Si phase, itself surrounded by a phase with another composition (which was not possible to determine by EDS). This phenomenon could be explained by considering the phase diagram. Indeed, after the eutectic crystallisation, SiU_3 forms by a peritectoid transition from U_3Si_2 grains. At a lower temperature, the peritectoid transition 'U_3Si + bcc-U = tetra-U' occurs. The phase surrounded U_3Si could be the tetragonal phase of uranium. Such phase could also correspond to the bcc-U phase Si depleted by the peritectoid reaction 'U_3Si_2 + bcc-U = U_3Si'. Although, due to the high cooling rate, no transition was evidenced for these two peritectoid transitions on the DTA thermograms. Such solid–solid transitions are controlled by diffusion. Presence of these two phases U_3Si and tetra-U after a relative high cooling (20 K/min) indicate high diffusion kinetic in these alloys.

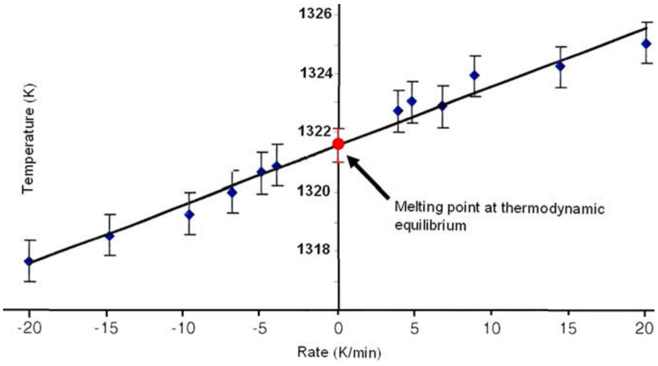

Fig. 2. Determination of the melting temperature of pure gold at the thermodynamic equilibrium.

3.3. U-46 at.% Si alloy

According to Vaugoyeau et al. [6], the composition of the liquid during the eutectic transition 'liquid = USi + U_3Si_2' (on cooling) is of 46 at.% Si at 1813 K. The temperature of the eutectic transition was measured at 1820 ± 5 K. Considering the experimental uncertainty;

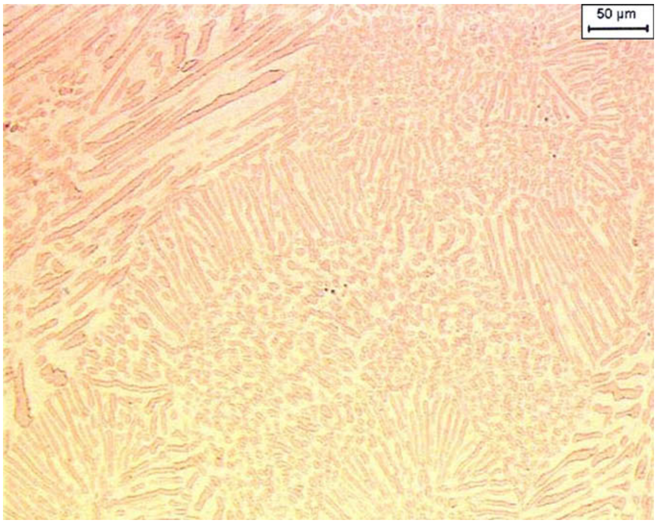

Fig. 3. Microstructure of the U-9 at.% Si sample cooled at 20 k/min.

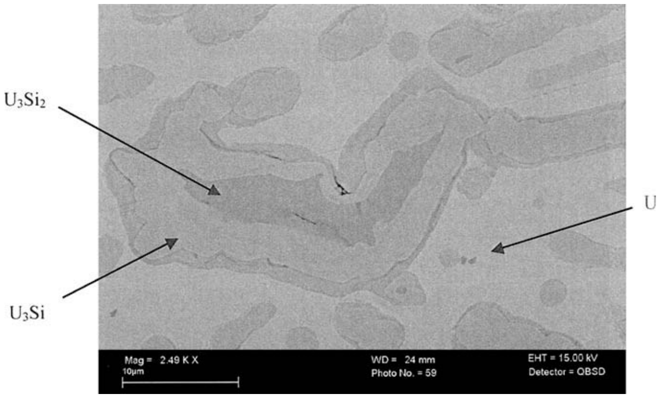

Fig. 4. Details of the eutectic structure of the U-9 at.% Si alloy cooled at 20 k/min revealed by SEM analysis.

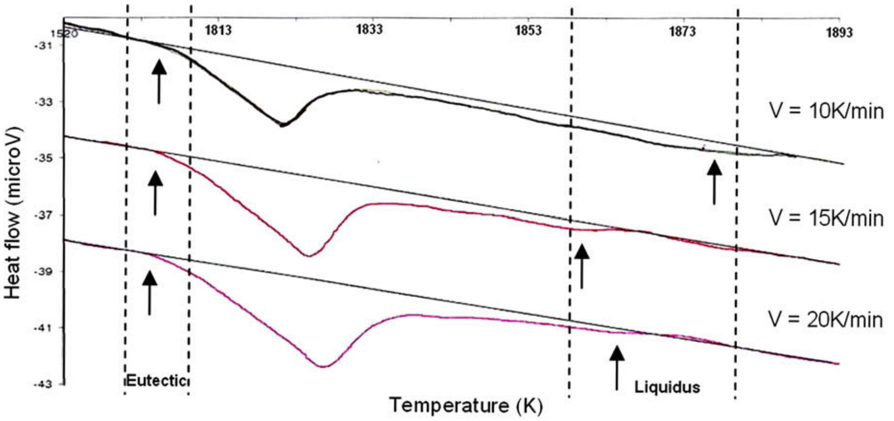

Fig. 5. DTA thermograms performed on U-46 at.% Si at different rate on heating.

this value is in very good agreement with the data of 1813 K proposed by Vaugoyeau et al. [6]. Although, DTA analysis performed on heating at different rates revealed the presence of a liquidus transition at 1867 ± 15 K (Fig. 5).

SEM analysis showed the presence of large primary crystallisation phase (Fig. 6) identified as U_3Si_2 by EDS surrounded by an eutectic zone (mainly constituted by USi with small precipitates). The crystals of U_3Si_2 primary phase are surrounded by a layer with a measured composition of 46 at.% Si. This phase may correspond to the U_5Si_4 compound found by Noel et al. [7]. Considering the present microstructure, the peritectic decomposition reaction [U_3Si_2 + liquid = U_5Si_4] is proposed. The analysis of the DTA thermograms does not allow determining accurately the temperature of this peritectic transition as the corresponding peak is not intense enough to be discriminated from the eutectic one. The temperature of 1840 K measured by Kaufman at a composition between U_5Si_4 and U_3Si_2 could correspond to this peritectic transition. From these results, the following transitions are proposed for the 46% at. Si alloy: the liquidus at 1867 ± 15 K, the peritectic reaction [U_3Si_2 +

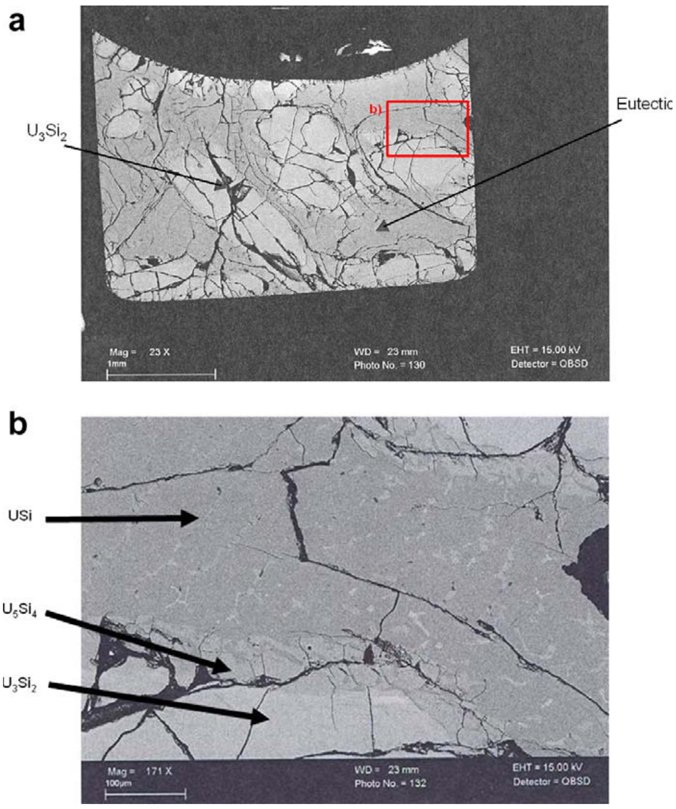

Fig. 6. (a) SEM picture of the U-46 at.% Si sample cooled at 20 K/min. Magnification of the (b) zone on the Fig. 6a.

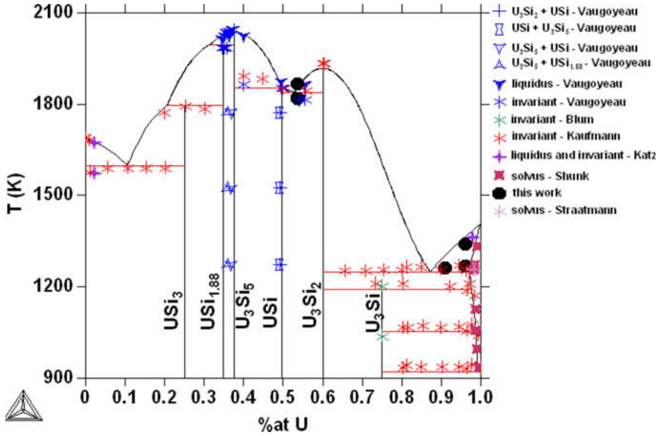

Fig. 7. Calculated Si–U phase diagram with experimental data (this work).

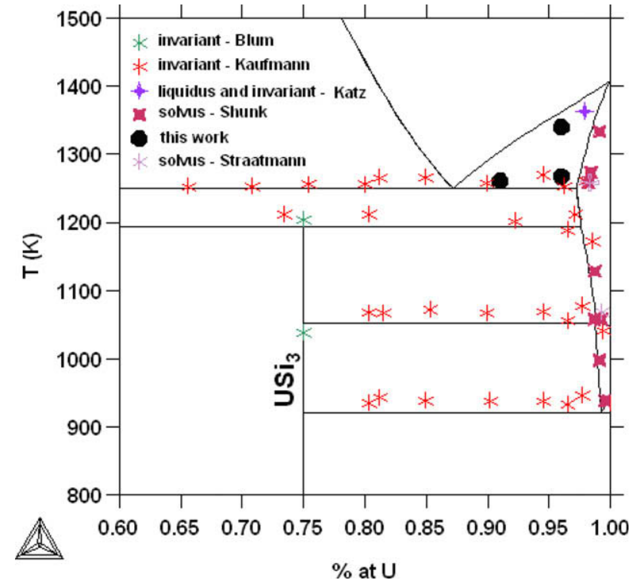

Fig. 8. Calculated Si–U phase diagram in the U enriched part with experimental data (this work).

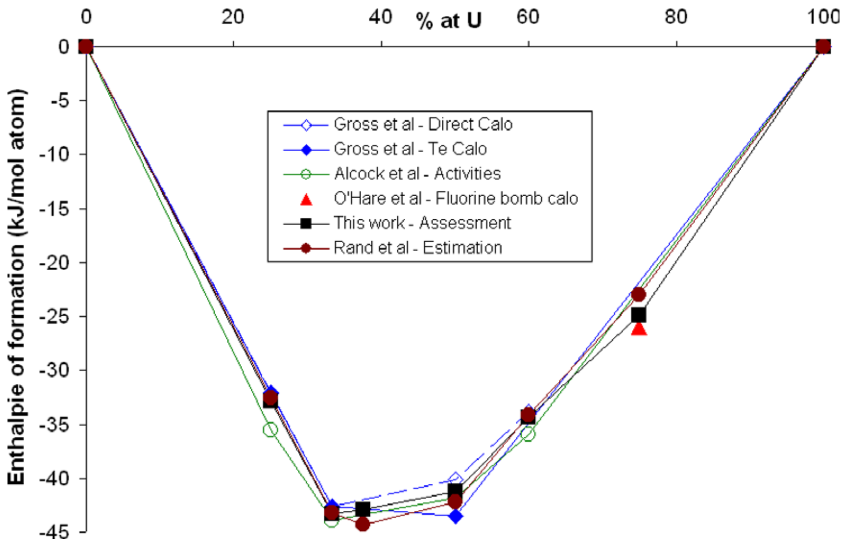

Fig. 9. Enthalpies of formation of the intermetallics phases determined in the literature compared to the calculation obtained from this assessment.

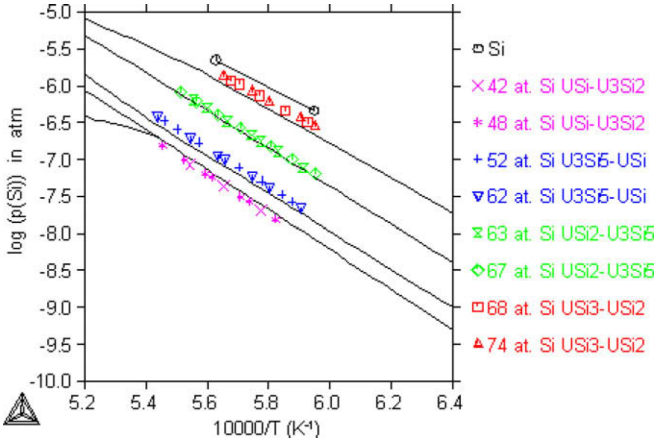

Fig. 10. Calculated of silicon partial pressure in Si–U system (this work)–comparison with Alcock's experimental data [14].

liquid = U_5Si_4] at 1840 K, and the eutectic reaction [liquid = U-Si + U_5Si_4] at 1820 ± 5 K.

4. Thermodynamic assessment

The calculated phase diagram is presented and compared with the experimental data in Figs. 7 and 8. An overall good agreement was obtained. However, the composition of the eutectic [liquid = -Si_2U_3 + bcc-U] is calculated at 13 at.% Si instead of 9 at.% Si as estimated in the first part. In fact, it was impossible to find a set of parameters that allows reproducing both the melting point of the Si_2U_3 compound and the eutectic composition of 9 at.% Si. These difficulties explain the large number of optimized excess parameters in the liquid phase. A higher weight was given to the melting point of Si_2U_3. New experimental measurements will be useful in this part of the phase diagram.

For the thermodynamic data, the calculated enthalpies of formation for all the compounds are listed in Table 1 and represented in the Fig. 9. The calculated partial pressures of silicon are

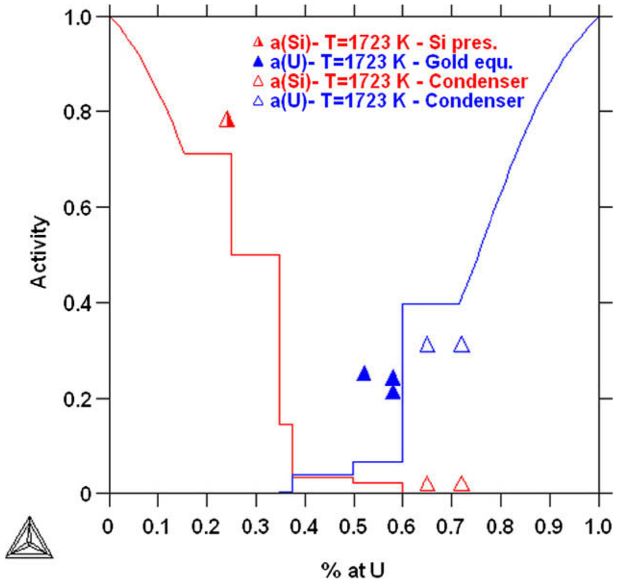

Fig. 11. Calculated Si and U activities at 1723 K (this work). Comparison with experimental data from Alcock and Grieveson [14].

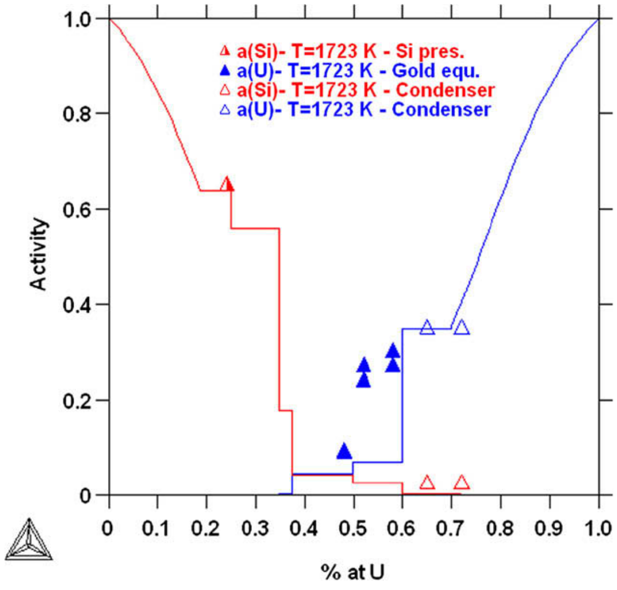

Fig. 12. Calculated Si and U activities at 1773 K (this work). Comparison with experimental data from Alcock and Grieveson [14].

Table 3
Optimized thermodynamic parameters for the Si–U system.

Phases	Thermodynamic parameters (J/mol)	References
Liquid (Si,U)	$G(liquid,Si) - {}^{\circ}H_{Si}^{SER} = G_{Si}^{liq}$	[17]
	$G(liquid,U) - {}^{\circ}H_{U}^{SER} = G_{Ui}^{liq}$	[17]
	$L_{(Si,U)}^{0} = -185537 + 26.42T$	Optimized
	$L_{(Si,U)}^{1} = -98478 + 53.79T$	Optimized
	$L_{(Si,U)}^{2} = +47133 - 16.79T$	Optimized
bcc (Si,U)$_1$(Va)$_3$	$G(bcc,Si) - {}^{\circ}H_{Si}^{SER} = G_{Si}^{bcc}$	[17]
	$G(bcc,U) - {}^{\circ}H_{U}^{SER} = G_{U}^{bcc}$	[17]
	$L_{(Si,U)_1(Va)_3}^{0} = -96137$	Optimized
Tetragonal (Si,U)	$G(tetra,Si) - {}^{\circ}H_{Si}^{SER} = G_{Si}^{diamond} + 5000$	Fixed
	$G(tetra,U) - {}^{\circ}H_{U}^{SER} = G_{U}^{tetragonal}$	[17]
	$L_{(Si,U)}^{0} = -78915.5$	Optimized
D0C_SiU$_3$(Si)$_1$(U)$_3$	$G(D0C\_SiU_3) - {}^{\circ}H_{Si}^{SER} - 3\,{}^{\circ}H_{U}^{SER} =$ $-99727 - 11.1T + G_{Si}^{diamond} + 3G_{U}^{orthor\,\mathrm{hom}\,bic}$	Optimized
D5A_Si$_2$U$_3$ (Si)$_2$(U)$_3$	$G(D5A\_Si_2U_3) - 2{}^{\circ}H_{Si}^{SER} - 3\,{}^{\circ}H_{U}^{SER} =$ $-171618 - 41.84T + 2G_{Si}^{diamond} + 3G_{U}^{orthor\,\mathrm{hom}\,bic}$	Optimized
SI$_{34.5}$U$_{34}$ (Si)$_{3.45}$(U)$_{3.4}$	$G(Si_{3.45}U_{3.4}) - 3.45\,{}^{\circ}H_{Si}^{SER} - 3.4\,{}^{\circ}H_{U}^{SER}$ $-282080 - 34.99T + 3.45G_{Si}^{diamond} + 3.4G_{U}^{orthor\,\mathrm{hom}\,bic}$	Optimized
C32_Si$_5$U$_3$ (Si)$_5$(U)$_3$	$G(C32\_Si_5U_3) - 5\,{}^{\circ}H_{Si}^{SER} - 3\,{}^{\circ}H_{U}^{SER} =$ $-343192 - 31.62T + 5G_{Si}^{diamond} + 3G_{U}^{orthor\,\mathrm{hom}\,bic}$	Optimized
C5_Si$_{1.88}$U (Si)$_{1.88}$(U)$_1$	$G(C5\_Si_{1.88}U) - 1.88\,{}^{\circ}H_{Si}^{SER} - {}^{\circ}H_{U}^{SER} =$ $-124792 - 8.06T + 1.88G_{Si}^{diamond} + G_{U}^{orthor\,\mathrm{hom}\,bic}$	Optimized
L12_Si$_3$U (Si)$_3$(U)$_1$	$G(L12\_Si_3U) - 3\,{}^{\circ}H_{Si}^{SER} - {}^{\circ}H_{U}^{SER} =$ $-131618 - 11.24T + 3G_{Si}^{diamond} + G_{U}^{orthor\,\mathrm{hom}\,bic}$	Optimized

compared to the experimental data from Alcock and Grieveson [14] in Fig. 10. A good agreement is obtained.

The calculated activities of U and Si are compared with the experimental data [14] at 1723 K in Fig. 11 and at 1773 K in Fig. 12. The plateaux correspond to the two-phase domains. Alcock and Grieveson deduced the activities in the two-phase domains using three different methods:

- Si and U activities from condenser experiments on U–U$_3$Si$_2$ mixtures;
- U activities from gold equilibration method (U activity is fixed by a U–Au alloy);
- Si activities from Si pressures measurements on USi$_3$–Si mixtures.

A good overall agreement is obtained except for the gold equilibration results for which the calculated data are three times lower than the experimental data. This discrepancy cannot be explained as a very good agreement is obtained for Si partial pressures and enthalpies of formation.

For the liquid, the calculated mixing enthalpy of −46.8 kJ/mol for 50 at.% Si at 2000 K is in good agreement with the estimations of Miedema et al. (−48.6 kJ/mol) [16].

The optimized parameters are listed in Table 3.

A first version of the U–Si database is obtained which is in good agreement with all the experimental data except for some U activities from Alcock and Grieveson [14]. The thermodynamic properties of the compounds are well known experimentally. The present description may be improved by the experimental determination of the following data:

- Liquidus temperatures for the whole system;
- The decomposition temperature of the U$_4$Si$_5$ compound (recently examined by Noel [7]);
- Additional activity measurements.

5. Conclusions

New measurements of liquidus temperatures have been carried out on the U–Si system. The temperature of two eutectic reactions was also confirmed in this work. Utilisation of Y_2O_{3-x} crucibles is suitable for silicon composition below 40–50 at.%. An assessment of the thermodynamic data for all the phases of the U–Si system is presented using the CALPHAD method. An overall good agreement is obtained but future experiments would be necessary to carry out, in order to fix the thermodynamic description of this important system.

Acknowledgments

SEM and EDS analyses were performed at DEN/DTEC/SGCS/LMAC.

References

[1] C. Guéneau, S. Chatain, S. Gossé, C. Rado, O. Rapaud, J. Lechelle, J.C. Dumas, C. Chatillon, J. Nucl. Mat. 344 (2005) 191.
[2] C. Guéneau, S. Chatain, J.C. Dumas, J. Lechelle, C. Rado, F. Defoort, N. Dupin, B. Sundman, H. Noel, R. Konings, FUELBASE: a thermodynamic database for advanced nuclear fuels, in: Proceedings HTR2006 : Third International Topical Meeting on High Temperature Reactor Technology, October 1–4 2006, Johannesburg, South Africa.
[3] C. Guéneau, N. Dupin, B. Sundman, C. Rado, R. Konings, A progress report on the development of FUELBASE, a thermodynamic database for the description of multicomponent systems for nuclear fuel applications. Part 1. Binary systems, Technical Report CEA/DEN/DANS/DPC/07-DO-31, DPC/SCP 07-224 indice A. February 2007.
[4] B.T. Massalski, Binary Alloy Phase Diagrams, second Ed., ASM, Materials Park, OH, 1990. pp. 3374–3375.
[5] A. Kaufmann, B. Cullity, G. Bitsianes, Trans. Amer. Inst. Min. Met. Eng. 209 (1957) 23.
[6] H. Vaugoyeau, L. Lombard, J.P. Morlevat, J. Nucl. Mater. 39 (1971) 323.
[7] H. Noel, V. Queneau, J.P. Durand, P. Colomb, in: Proceedings of the International Conference on Strongly Correlated Electron Systems, July 15–18, 1998, Paris.
[8] P.L. Blum, G. Silvestre, H. Vaugoyeau, Acad. Sci. Paris t 260 (1965) 5538.
[9] F.A. Shunk, Constitution of Binary Alloys, Second Supplement, McGraw-Hill Book Company, 1969.
[10] A. Straatmann, N.F. Neumann, Reast. Mater. 8 (2) (1965) 57.
[11] J. Katz, E. Rabinowitch, The Chemistry of Uranium, Dover Publications 34, Inc., New York, 1951.
[12] P. Gross, C. Hayman, H. Clayton, Thermodynamics of Nuclear Materials, IAEA, Vienna, 1962. pp. 653–665.
[13] P.A.G. O'Hare et al., Thermodynamics of Nuclear Materials, I.A.E Vienne, vol. 2, 1975, pp. 439–453.
[14] C. Alcock, P.J. Grieveson, J. Inst. Metals 90 (1962) 304.
[15] M.H. Rand, O. Kubaschewski, The Thermochemical Properties of Uranium Compounds, Oliver & Boyd, Edinburgh, London, 1963. pp. 46–47.

[16] A.R. Miedema, P.F. de Chatel, F.R. de Boer, Physica 100B (1980) 1. results from the program PTP version 4.0 implemented by Dr. K.C. Hari Kumar, Department MTM, Katholieke Universiteit Leuven, W. de Croylaan 2, B-3001 Leuven (Heverlee) BELGIUM and Dr. Toshihiro Tanaka, Department of Materials Science & Processing Faculty of Engg., Osaka University Suita, OSAKA 565, JAPAN, 1994..
[17] A. Dinsdale, CALPHAD 15 (1991) 317.